JBIC Journal of Biological Inorganic Chemistry
https://doi.org/10.1007/s00775-018-1634-9

ORIGINAL PAPER

Novobiocin–ferrocene conjugates possessing anticancer and antiplasmodial activity independent of HSP90 inhibition

Mziyanda Mbaba[1] · Jo-Anne de la Mare[2,3,4] · Jason N. Sterrenberg[2,3] · Deborah Kajewole[2,3] · Shantal Maharaj[2,3] · Adrienne L. Edkins[2,3,4] · Michelle Isaacs[4] · Heinrich C. Hoppe[2,3,4] · Setshaba D. Khanye[1,4,5]

Received: 28 September 2018 / Accepted: 4 December 2018
© Society for Biological Inorganic Chemistry (SBIC) 2018

Abstract

A series of tailored novobiocin–ferrocene conjugates was prepared in moderate yields and investigated for in vitro anticancer and antiplasmodial activity against the MDA-MB-231 breast cancer line and *Plasmodium falciparum* 3D7 strain, respectively. While the target compounds displayed moderate anticancer activity against the breast cancer cell line with IC_{50} values in the mid-micromolar range, compounds **10a–c** displayed promising antiplasmodial activity as low as 0.889 µM. Furthermore, the most promising compounds were tested for inhibitory effects against a postulated target, heat shock protein 90 (Hsp90).

Graphical abstract A selection of tailored novobiocin derivatives bearing the organometallic ferrocene unit were synthesized and characterized by common spectroscopic techniques. The target compounds were investigated for in vitro anticancer and antimalarial activity against the MDA-MB-231 breast cancer cell line and *Plasmodium falciparum* 3D7 strain, respectively.

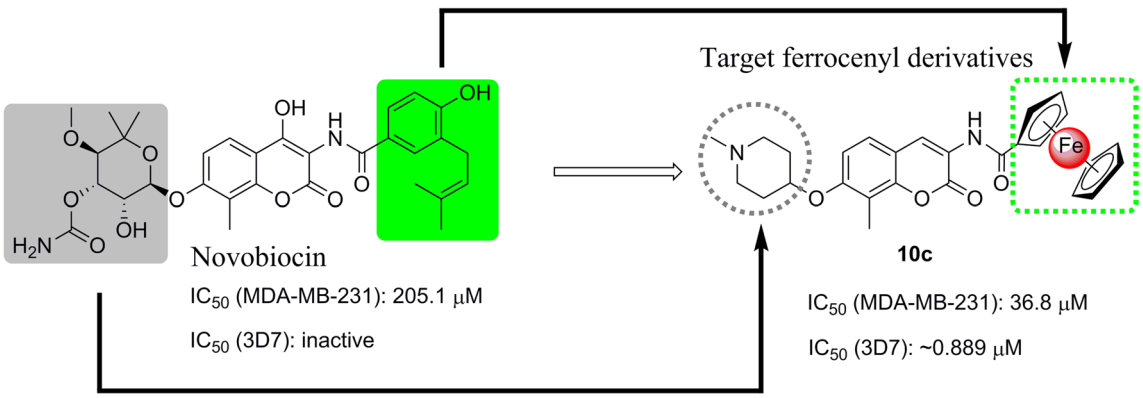

Keywords Novobiocin · Coumarin · Ferrocene · Heat shock protein 90 · Hsp90 · Breast cancer · *Plasmodium falciparum*

Introduction

The development of resistance to clinically approved anticancer and antimalarial drugs has intensified research endeavours towards the search for novel drug targets and bioactive compounds. Novobiocin (**1**) is an antibiotic isolated from *Streptomyces* bacteria and is a weak inhibitor of the chaperone, heat shock protein 90 (Hsp90) [1]. Novobiocin derivatives have shown promise as anticancer agents

Electronic supplementary material The online version of this article (https://doi.org/10.1007/s00775-018-1634-9) contains supplementary material, which is available to authorized users.

✉ Mziyanda Mbaba
mziyanda.mbaba@gmail.com

✉ Setshaba D. Khanye
s.khanye@ru.ac.za

Extended author information available on the last page of the article

Published online: 12 December 2018

by inhibiting the function of this chaperone [2–4]. Within the cell, Hsp90 is responsible for the stabilisation and conformational regulation of polypeptides to support the attainment of their functional forms [5]. Numerous proteins stabilised by Hsp90, i.e., Hsp90 client proteins including cell signalling proteins, steroid hormone receptors and regulatory kinases, are involved in essential cellular processes [6]. Hence, Hsp90 is crucial for normal cell function as it mediates these processes by maturing the proteins involved. As a result, the chaperone bears therapeutic potential as a drug target [7, 8].

In cancer, Hsp90 is associated with the manifestation of the oncogenic phenotype [9–12]. It is central to the hallmarks pertaining the oncogenic phenotype as several of the corresponding client proteins are associated with each of these traits [11]. The research groups of Blagg and Alami have extensively explored the inhibition of the C-terminal domain of the Hsp90 by organic novobiocin derivatives and have demonstrated that these induce antiproliferative effects in cancer cell lines [13–16]. More importantly, these studies revealed that the replacement of the benzamide (RHS = right-hand side) and noviose (LHS = left-hand side) moieties of **1** with simpler structural motifs retains the anticancer efficacy of the resulting compounds [13–16]. Some examples of tailored novobiocin derivatives with promising anticancer activity are displayed in Fig. 1 [13–17].

Similarly, Hsp90 has been shown to play a vital role in the life-cycle of the parasite, *Plasmodium falciparum*, which causes cerebral malaria [9, 10, 12]. Previous studies by Banumathy and co-workers revealed the significance of *P. falciparum* Hsp90 (*Pf*Hsp90) in the development of the parasite by demonstrating that the N-terminal Hsp90 inhibitor geldanamycin suppressed the growth of the parasite in vitro [10]. It has also been postulated that *Pf*Hsp90 mediates pro-survival mechanisms of the parasite in stressful environments like drug-induced stress, thereby potentiating drug resistance [12, 18]. *Pf*Hsp90 is considered to be an appealing drug target in malaria, and the antimalarial activity of a group of aminoalcohol-carbazoles and 7-azaindole compounds is due to their ability to inhibit this protein [19, 20]. In addition, selected analogues of the beta-carboline alkaloid harmine that bound *Pf*Hsp90 inhibited the growth of *P. falciparum* W2 strain in vitro and were active against *Plasmodium berghei* in vivo [21]. These compounds significantly increased the sensitivity of *Plasmodium* parasites to the antimalarial agent dihydroartemisinin [21]. A significant number of studies have demonstrated **1** to modestly suppress the growth of selected strains of *P. falciparum* in vitro [22, 23]. Despite the evidence underpinning the importance of Hsp90 in *P. falciparum* growth and the antimalarial activity of **1**, there are no reports in literature regarding the exploration of *Pf*Hsp90 as a therapeutic target of compounds based on the chemical scaffold of **1**.

The incorporation of organometallic units into biologically active scaffolds has been hailed as an attractive strategy in the field of medicinal chemistry in the quest for novel compounds with efficacy against various diseases [24–26]. Most auspicious in this application is the organometallic unit, ferrocene, which has attracted great interest in drug discovery owing to its appealing medicinal attributes such as high aromaticity, lipophilicity, chemical stability, favourable redox behaviour, ability to form reactive oxygen species (ROS) and absence of cytotoxicity in human cells [27, 28]. The success of ferrocene in drug discovery is best represented by ferroquine (FQ, SSR97193), an efficacious chloroquine–ferrocene conjugate currently in phase II clinical trials for treatment of malaria [29]. Moreover, the pioneering work of Jaouen and co-workers on anti-tumour ferrocifens which are modelled on the tamoxifen scaffold has led to the development of a substantial number of ferrocifen type anticancer drugs possessing different modes of action against

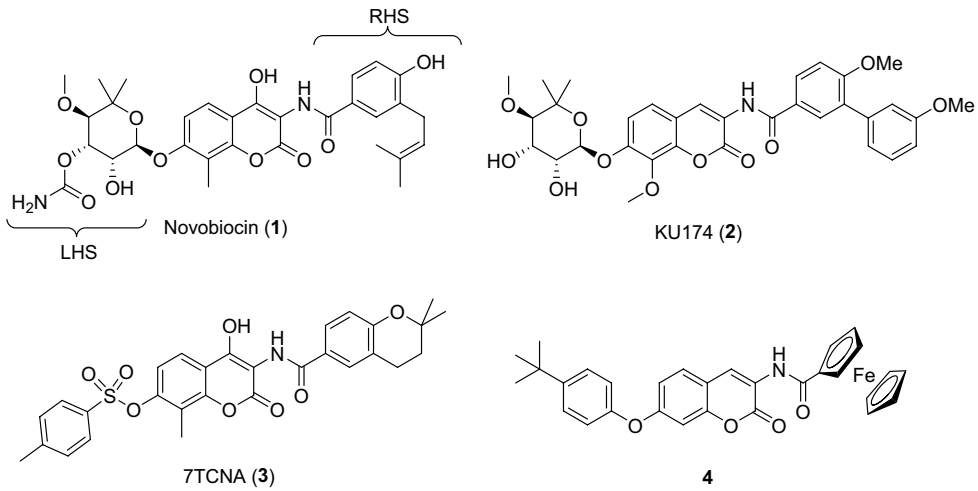

Fig. 1 Chemical structures of novobiocin (**1**) and its simplified derivatives **2**–**4** possessing anticancer activity. *LHS* left-hand side, *RHS* right-hand side

various cancer cells and, thus, bear potential of circumventing resistance [30, 31].

Previously, we demonstrated that the incorporation of the organometallic ferrocene unit into the novobiocin framework led to compounds such as **4** (Fig. 1) with enhanced activity against the HCC38 breast cancer cell line and chloroquine-sensitive 3D7 strain of the *P. falciparum* parasite [17]. Furthermore, the resultant ferrocenyl novobiocin derivatives contained phenyl substituents in lieu of the structurally complex noviose appendage on the LHS. In an effort to further investigate the pharmacological profile of these derivatives, in this work we explored the potential activity of ferrocenyl derivatives of **1** containing simpler structural units (e.g., benzyl and piperidine) devoid of the complex noviose moiety at C-7 of the coumarin core. We also sought to ascertain if the observed anticancer and antiplasmodial efficacies of pursued compounds are attributable to inhibition of the chaperone Hsp90 by screening the inhibitory activity of the most promising compounds against human and *P. falciparum* Hsp90 isoforms, namely *Hs*Hsp90β and *Pf*Hsp90.

Materials and methods

Materials

All chemical reagents and solvents used in this study were sourced from Merck (Pty) Ltd. and were used without further purification. The progress of each reaction was monitored by analytical thin-layer chromatography (TLC) using Merck F_{254} silica gel plates (supported on aluminium sheets) and the plates were visualised under ultraviolet light (UV 254 and 366 nm) and in an iodine flask. Where necessary, the crude compounds were purified by silica gel column chromatography using Merck Kieselgel 60 Å: 70–230 (0.068–0.2 mm) silica gel mesh.

Instrumentation

The ^{1}H and ^{13}C NMR spectra were recorded on Bruker Biospin 300, 400 or 600 MHz spectrometers, and were referenced internally using residual solvent signals of DMSO-d_6: 2.50 ppm for ^{1}H NMR and 39.5 ppm for ^{13}C NMR, or $CDCl_3$: 7.26 ppm for ^{1}H NMR and 77.2 ppm for ^{13}C NMR at ambient temperature. The high-resolution mass spectra (HRMS) were recorded on Waters Synapt G2 Mass Spectrometer (Central Analytical Facility, University of Stellenbosch) using electron spray ionization (ESI) in the positive ionization mode, and the IR spectra were recorded on PerkinElmer Spectrum 100 FT-IR Spectrometer in the mid-IR range (640–4000 cm^{-1}). The melting points were determined using the Reichert melting point apparatus and were uncorrected.

Preparation of compounds: general procedure for synthesis of 10a–f [15]

An appropriate volume of diisopropyl azodicarboxylate (DIAD) (2.0 eq.) was added to a suspension of a relevant phenolic substrate **8a**–**b** (1.0 eq.), piperidinol (**9a**–**d**) (1.0 eq.) and triphenylphosphine (PPh_3) (2.0 eq.) in THF (20 mL) on ice. The reaction mixture was stirred at 0°C for 5 h followed by removal of the solvent under reduced pressure. The resulting orange residue was purified by silica gel chromatography (5% MeOH/DCM) to afford the desired product **10a**–**f**.

7-(*N*-methyl-4-piperidinyl)-*O*-3-ferrocenylcarboxamidocoumarin (10a)

7-Hydroxy-3-ferrocenylcarboxamidocoumarin **8a** (0.100 g, 0.26 mmol), **9a** (0.030 g, 0.26 mmol), PPh_3 (0.135 g, 0.51 mmol) and DIAD (0.104 g, 0.51 mmol) afforded **10a** as a red solid (0.051 g, 41%). M.p.: 161–163°C. IR ν_{max}/cm^{-1}: 3355 (N–H, amide), 3107 (C–H, pyrone HC = C), 2935 (C–H, methyl), 1704 (C = O, lactone), 1659 (C = O, amide), 1501 (C = C, aromatic), 1173 (C–O, aromatic ether); ^{1}H NMR (600 MHz, $CDCl_3$): δ 8.68 (s, 1H, NH), 8.25 (s, 1H, −HC = C−), 7.40 (d, J = 8.6 Hz, 1H, ArH), 6.89 (dd, J = 8.6, 2.4 Hz, 1H, ArH), 6.85 (d, J = 2.4 Hz, 1H, ArH), 4.82 (t, J = 1.9 Hz, 2H, FcH), 4.46 (t, J = 1.9 Hz, 2H, FcH), 4.39 (br s, 1H, CH), 4.26 (s, 5H, FcH), 2.73 (s, 2H, CH_2), 2.34 (br s, 5H, CH_2, CH_3), 2.09–2.04 (m, 2H, CH_2), 1.92–1.87 (m, 2H, CH_2); ^{13}C NMR (150 MHz, $CDCl_3$): δ 170.0, 159.5, 159.1, 151.5, 128.8, 123.4, 122.1, 114.6, 113.6, 102.8, 75.4, 71.5 (2C), 70.2 (5C), 68.6 (2C), 53.6 (2C), 46.1, 30.4 (2C), 29.9; HRMS (ESI^+) *m/z* calcd for $C_{26}H_{26}FeN_2O_4$: 486.1242; found: 487.1318 $[M+H]^+$.

7-(*N*-methyl-3-piperidinyl)-*O*-3-ferrocenylcarboxamidocoumarin (10b)

7-Hydroxy-3-ferrocenylcarboxamidocoumarin **8a** (0.100 g, 0.26 mmol), **9b** (0.030 g, 0.26 mmol), PPh_3 (0.135 g, 0.51 mmol) and DIAD (0.104 g, 0.51 mmol) afforded **10b** as a red solid (0.046 g, 37%). M.p.: 161–163°C. IR ν_{max}/cm^{-1}: 3380 (N–H, amide), 3068 (C–H, pyrone HC = C), 2923 (C–H, methyl), 1706 (C = O, lactone), 1663 (C = O, amide), 1518 (C = C, aromatic), 1237 (C–O, aromatic ether); ^{1}H NMR (600 MHz, $CDCl_3$): δ 8.68 (s, 1H, NH), 8.25 (s, 1H, –HC = C–), 7.40 (d, J = 8.6 Hz, 1H, ArH), 6.92 (dd, J = 8.6, 1.9 Hz, 1H, ArH), 6.89 (d, J = 1.6, 1H, ArH), 4.82 (br s, 2H, FcH), 4.46–4.44 (m, 3H, FcH and CH), 4.26 (s, 5H, FcH), 2.91–2.58 (m, 2H, CH_2), 2.32–2.17 (m, 5H, CH_3 and CH_2), 2.05–1.84 (m, 2H, CH_2), 1.68–1.54 (m, 2H, CH_2); ^{13}C NMR (150 MHz, $CDCl_3$): δ 170.3, 159.8, 159.6, 151.7, 129.1, 123.8, 122.3, 114.8, 113.9, 103.1, 75.7, 73.7, 71.8

(2C), 70.5 (5C), 68.9 (2C), 59.9, 55.8, 46.8, 29.3, 23.2; HRMS (ESI$^+$) *m/z* calcd for $C_{26}H_{26}FeN_2O_4$: 486.1242; found 487.1328 $[M+H]^+$.

7-(*N*-methyl-4-piperidinyl)-*O*-8-methyl-3-ferrocenylcarboxamidocoumarin (10c)

7-Hydroxy-8-methyl-3-ferrocenylcarboxamidocoumarin **8b** (0.060 g, 0.15 mmol), **9a** (0.017 g, 0.15 mmol), PPh_3 (0.078 g, 0.30 mmol) and DIAD (0.060 g, 0.30 mmol) afforded **10c** as a red solid (0.016 g, 22%). M.p.: 161–163°C. IR ν_{max}/cm^{-1}: 3363 (N–H, amide), 3079 (C–H, pyrone HC = C), 2921 (C–H, methyl), 1704 (C = O, lactone), 1658 (C = O, amide), 1521 (C = C, aromatic), 1107 (C–O, aromatic ether); ^{1}H NMR (600 MHz, $CDCl_3$): δ 8.67 (s, 1H, NH), 8.27 (s, 1H, –HC = C–), 7.29 (d, J = 8.6 Hz, 1H, ArH), 6.87 (d, J = 8.6 Hz, 1H, ArH), 4.85–4.82 (m, 2H, FcH), 4.49–4.43 (m, 3H, FcH and CH), 4.26 (s, 5H, FcH), 2.66 (s, 2H, CH_2), 2.38 (s, 2H, CH_2) 2.35 (s, 3H, CH_3), 2.33 (s, 3H, CH_3), 2.07–1.99 (m, 2H, CH_2), 1.95–1.87 (m, 2H, CH_2); ^{13}C NMR (150 MHz, $CDCl_3$): δ 169.9, 159.7, 156.9, 149.5, 125.5, 123.9, 121.7, 115.4, 113.6, 110.7, 75.4, 71.5 (2C), 70.2 (5C), 68.5 (2C), 52.5 (2C), 46.4, 30.9 (2C), 29.8, 8.5; HRMS (ESI$^+$) *m/z* calcd for $C_{27}H_{28}FeN_2O_4$: 500.1398; found 501.1471 $[M+H]^+$.

7-(*N*-methyl-3-piperidinyl)-*O*-8-methyl-3-ferrocenylcarboxamidocoumarin (10d)

7-Hydroxy-8-methyl-3-ferrocenylcarboxamidocoumarin **8b** (0.060 g, 0.15 mmol), **9b** (0.017 g, 0.15 mmol), PPh_3 (0.078 g, 0.30 mmol) and DIAD (0.060 g, 0.30 mmol) afforded **10d** as a red solid (0.016 g, 38%). M.p.: 100–102°C. IR ν_{max}/cm^{-1}: 3361 (N–H, amide), 3088 (C–H, pyrone HC = C), 2925 (C–H, methyl), 1702 (C = O, lactone), 1660 (C = O, amide), 1517 (C = C, aromatic), 1107 (C–O, aromatic ether); ^{1}H NMR (300 MHz, $CDCl_3$): δ 8.67 (s, 1H, NH), 8.27 (s, 1H, –HC = C–), 7.31 (d, J = 8.6 Hz, 1H, ArH), 6.97 (d, J = 8.7 Hz, 1H, ArH), 4.83 (t, J = 1.95 Hz, 2H, FcH), 4.56 (br s, 1H, CH), 4.46 (t, J = 1.95 Hz, 2H, FcH), 4.2 (s, 5H, FcH), 3.19–2.80 (m, 2H, CH_2), 2.42–2.32 (m, 3H, CH_3), 2.30 (s, 3H, CH_3), 2.17 (s, 3H, CH_3), 1.90–1.80 (m, 3H, CH_3); ^{13}C NMR (150 MHz, $CDCl_3$): δ 170.0, 159.7, 156.7, 149.4, 125.7, 123.8, 121.8, 115.5, 114.0, 111.1, 75.4, 71.5 (2C), 70.2 (5C), 68.6 (2C), 55.3, 53.6, 46.0, 31.1, 29.9, 22.1, 8.6; HRMS (ESI$^+$) *m/z* calcd for $C_{27}H_{28}FeN_2O_4$: 500.1398; found 501.1474 $[M+H]^+$.

7-(*N*-Boc-4-piperidinyl)-*O*-3-ferrocenylcarboxamidocoumarin (10e)

7-Hydroxy-3-ferrocenylcarboxamidocoumarin **8a** (0.100 g, 0.26 mmol), **9c** (0.052 g, 0.26 mmol), PPh_3 (0.135 g, 0.51 mmol) and DIAD (0.104 g, 0.51 mmol) afforded **10e** as a red solid (0.055 g, 37%). M.p.: 159–161°C. IR ν_{max}/cm^{-1}: 3399 (N–H, amide), 3089 (C–H, pyrone HC = C), 2934 (C–H, methyl), 1692 (C = O, lactone), 1662 (C = O, amide), 1520 (C = C, aromatic), 1234 (C–O, aromatic ether); ^{1}H NMR (600 MHz, $CDCl_3$): δ 8.69 (s, 1H, NH), 8.26 (s, 1H, –HC = C–), 7.42 (d, J = 8.6 Hz, 1H, ArH), 6.89 (dd, J = 8.6, 2.4 Hz, 1H, ArH), 6.86 (d, J = 2.3 Hz, 1H, ArH), 4.82 (t, J = 1.8 Hz, 2H, FcH), 4.55–4.51 (m, 1H, CH), 4.47 (t, J = 1.8 Hz, 2H, FcH), 4.26 (s, 5H, FcH), 3.73–3.69 (m, 2H, CH_2), 3.39–3.35 (m, 2H, CH_2), 1.97–1.95 (m, 2H, CH_2), 1.81–1.77 (m, 2H, CH_2), 1.47 (s, 9H, *tert*-butyl); ^{13}C NMR (150 MHz, $CDCl_3$): δ 170.0, 167.6, 159.4, 158.9, 155.0, 151.4, 128.9, 123.4, 122.1, 114.7, 113.7, 102.8, 80.0 (2C), 77.5, 73.1 (2C), 71.6 (2C), 70.3 (5C), 68.6 (2C), 28.6 (3C), 21.9; HRMS (ESI$^+$) *m/z* calcd for $C_{30}H_{32}FeN_2O_6$: 572.1610; found 494.1045 $[C_{25}H_{23}FeN_2O_4+Na]^+$.

7-(*N*-Boc-3-piperidinyl)-*O*-3-ferrocenylcarboxamidocoumarin (10f)

7-Hydroxy-3-ferrocenylcarboxamidocoumarin **8a** (0.100 g, 0.26 mmol), **9d** (0.052 g, 0.26 mmol), PPh_3 (0.135 g, 0.51 mmol) and DIAD (0.104 g, 0.51 mmol) afforded **10f** as a red solid (0.060 g, 40%). M.p.: 112–114°C. IR ν_{max}/cm^{-1}: 3384 (N–H, amide), 3056 (C–H, pyrone HC = C), 2926 (C–H, methyl), 1698 (C = O, lactone), 1663 (C = O, amide), 1518 (C = C, aromatic), 1232 (C–O, aromatic ether); ^{1}H NMR (400 MHz, $CDCl_3$): δ 8.68 (s, 1H, NH), 8.27 (s, 1H, –HC = C–), 7.41 (d, J = 8.6 Hz, 1H, ArH), 7.05 (d, J = 2.2 Hz, 1H, ArH), 6.99 (dd, J = 8.6, 2.2 Hz, 1H, ArH), 5.14–4.94 (m, 1H, CH), 4.82 (t, J = 1.29 Hz, 2H, FcH), 4.46 (t, J = 1.26 Hz, 2H, FcH), 4.26 (s, 5H, FcH), 4.08–3.95 (m, 2H, CH_2), 2.31–2.09 (m, 4H, 2 × CH_2), 2.04–1.94 (m, 2H, CH_2), 1.47 (s, 9H, *tert*-butyl); ^{13}C NMR (100 MHz, $CDCl_3$): δ 169.8, 159.3, 158.6, 151.0, 128.4, 123.3, 122.0, 114.7, 113.9, 103.9, 102.6, 75.2, 71.3 (2C), 70.1 (5C), 68.5 (2C), 68.4 (3C), 32.7, 28.4 (3C), 23.3 (2C); HRMS (ESI$^+$) *m/z* calcd for $C_{30}H_{32}FeN_2O_6$: 572.1610; found 373.1765 $[C_{20}H_{15}FeNO_3+H]^+$.

General procedure for synthesis of compounds 10g–h [15]

A relevant *N*Boc-protected piperidinyl derivative **10e–f** (1.0 eq.) was stirred in 10% TFA/DCM solution (2 mL) for 12 h at room temperature. The solvents were removed under reduced pressure to obtain a crude product, which was purified by silica gel column chromatography (10% MeOH/DCM) to afford the desired product **10g–h**.

7-(4-Piperidinyl)-*O*-3-ferrocenylcarboxamidocoumarin (10g)

7-(*N*-Boc-4-piperininyl)-*O*-3-ferrocenylcarboxamidocoumarin **10e** (0.045 g, 0.079 mmol) and 10% TFA/DCM solution (2 mL) afforded **10g** as a light red solid (0.035 g, 95%). Mp.: 76–80°C. IR ν_{max}/cm^{-1}: 3397 (N–H, amide and piperidinyl amine), 2931 (C–H, pyrone HC = C), 2708 (C–H, methyl), 1658 (C = O, lactone), 1610 (C = O, amide), 1530 (C = C, aromatic), 1131 (C–O, aromatic ether); ^{1}H NMR (300 MHz, $CDCl_3$): δ 8.69 (s, 1H, NH), 8.26 (s, 1H, –HC = C–), 7.45 (d, J = 8.6 Hz, 1H, ArH), 6.90 (dd, J = 8.6, 2.2 Hz, 1H, ArH), 6.85 (d, J = 1.7 Hz, 1H, ArH), 4.82 (t, J = 1.8 Hz, 2H, FcH), 4.72 (br s, 1H, CH), 4.47 (t, J = 1.8 Hz, 2H, FcH), 4.26 (s, 5H, FcH), 3.31 (br s, 4H, 2 × CH_2), 2.19 (br s, 4H, 2 × CH_2); ^{13}C NMR (75 MHz, $CDCl_3$): δ 170.0, 159.5, 159.3, 151.4, 128.8, 123.5, 122.1, 114.5, 113.6, 102.8, 75.4, 73.4, 71.5 (2C), 70.2 (5C), 68.5 (2C), 59.6 (2C), 55.5 (2C); HRMS (ESI^+) *m/z* calcd for $C_{25}H_{24}FeN_2O_4$: 472.1085; found 473.1156 $[M + H]^+$.

7-(3-Piperidinyl)-*O*-3-ferrocenylcarboxamidocoumarin (10h)

7-(*N*-Boc-3-piperininyl)-*O*-3-ferrocenylcarboxamidocoumarin **10f** (0.045 g, 0.079 mmol) and 10% TFA/DCM solution (2 mL) afforded **10h** as a light red solid (0.036 g, 97%). Mp.: > 300°C. IR ν_{max}/cm^{-1}: 3385 (N–H, amide and piperidinyl amine), 2920 (C–H, pyrone HC = C), 1702 (C = O, lactone), 1607 (C = O, amide), 1607 (C = C, aromatic), 1533 (C–O, ether); ^{1}H NMR (300 MHz, $CDCl_3$): δ 8.68 (s, 1H, NH), 8.26 (s, 1H, –HC = C–), 7.40 (d, J = 8.7 Hz, 1H, ArH), 7.04 (d, J = 2.3 Hz, 1H, ArH), 6.98 (dd, J = 8.6, 2.4 Hz, 1H, ArH), 5.89–5.80 (m, 1H, NH), 4.82 (t, J = 1.92 Hz, 2H, FcH), 4.46 (t, J = 1.92, 2H, FcH), 4.34–4.31 (m, 1H, CH), 4.26 (s, 5H, FcH), 4.06–3.92 (m, 2H, CH_2), 2.52–1.92 (m, 6H, 3 × CH_2); ^{13}C NMR (75 MHz, $CDCl_3$): δ 170.0, 159.5, 158.8, 151.1, 128.6, 123.5, 122.1, 114.8, 114.0, 102.7, 75.3, 71.5 (2C), 70.2 (5C), 68.6, 68.5 (3C), 32.9, 28.0, 23.5; HRMS (ESI^+) *m/z* calcd for $C_{25}H_{24}FeN_2O_4$: 472.1085; found 473.3404 $[M + H]^+$.

Biological assays

MDA-MB-231 breast cancer cell line toxicity and analysis of Hsp90 inhibition

The MDA-MB-231 human triple negative breast adenocarcinoma cell line (ATCC HTB-26) was maintained in culture in L-15 media supplemented with 10% (v/v) heat-inactivated foetal bovine serum (FBS), 1 mM L-glutamine, 100 U/mL penicillin, 100 µg/mL streptomycin and 12.5 µg/mL amphotericin (PSA) at 37 °C and 9% CO_2. The toxicity of novobiocin derivatives and the reference compounds (**1** and Paclitaxel) was assessed in this cell line using a WST-1 cell proliferation kit (Roche, South Africa) conducted according to the manufacturer's instructions. Cells were seeded at equal density (1.2×10^5 cells/mL at 50 µL/well) in a 96-well plate and treated the following day with a range of compound concentrations (0, 0.32, 1.6, 8, 40, 200, 1000 µM) in triplicate. After 96 h, media-containing compounds were removed from the wells and 5 µL of a 5-mg/mL WST-1 reagent in 100 µL of medium was added to each of the wells and incubated for 4 h prior to reading absorbance at 450 nm in a Powerwave spectrophotometer (Biotek, South Africa). The dose response and half-maximal inhibitory concentrations (IC_{50}) were determined by non-linear regression using GraphPad Prism 4 software.

For the mammalian cell line Hsp90 inhibition assay, MDA-MB-231 cells (5×10^5) were treated with vehicle control (0.1% DMSO), compounds **10a** and **10g** (100 µM) or Hsp90 inhibitors: 17-dimethylaminoethylamino-17-demethoxygeldanamycin (17-DMAG; Alvespimycin, 10 µM) or novobiocin (NOV, 100 µM) for 24 h. Equal amounts of cell lysates were resolved by SDS-PAGE and the levels of Hsp90, Hsp70 or cyclin-dependent kinase 4 (CDK4) determined by Western blot analysis according to standard protocols [32, 33]. Glyceraldehyde 3-phosphate dehydrogenase (GAPDH) was used as a loading control.

In vitro antiplasmodial assay

The *P. falciparum* parasites (3D7 strain) were routinely cultured in a medium consisting of RPMI1640 containing 25 mM HEPES (Lonza, South Africa), 0.5% (w/v) Albumax II (Thermo Fisher Scientific, South Africa), 22 mM glucose, 0.65 mM hypoxanthine, 0.05 mg/mL gentamicin and 2–4% (v/v) human erythrocytes and were maintained at 37°C under an atmosphere of 5% CO_2, 5% O_2 and 90% N_2. The antiplasmodial activity of test compounds was assessed using a colorimetric assay as previously described [34].

In vitro HeLa cell cytotoxicity assay

HeLa cells (Cellonex, South Africa) were cultured in Dulbecco's Modified Eagle's medium (Lonza, South Africa) supplemented with 10% foetal calf serum and antibiotics (penicillin, streptomycin and amphotericin B) in a 5% CO_2 incubator maintained at 37°C. Following seeding of HeLa cells into 96-well plates and incubation for 24 h, the test compounds were added to a final concentration of 20 µM and cell viability was surveyed using a previously described resazurin fluorescence assay [35].

Yeast assay for Hsp90 inhibition

Yeast strains lacking *Saccharomyces cerevisiae* Hsp82 and expressing *Homo sapiens* Hsp90β (DP584) and *P. falciparum* Hsp90 (DP553) were donated by the laboratory of Prof. Didier Picard (University of Geneva, Switzerland) [36]. Strains were grown in YEP broth [10 g/L yeast extract, 20 g/L peptone, 2% (w/v) glucose and 40 µg/mL adenine] and on YEP agar [YEP broth supplemented with 2% (w/v) agar] and maintained using standard techniques. For growth inhibition assays, YEP agar was supplemented with 1 mM of geldanamycin (GA), novobiocin (**1**), compound **10a**, compound **10g** or dimethylsulfoxide (DMSO) as the vehicle control. Four tenfold dilutions were made with strains growing at mid-logarithmic phase (OD600 of 0.8). Cell dilutions (undiluted, and 10^{-1}, 10^{-2}, 10^{-3} and 10^{-4} dilutions) were spotted onto each of the compound-containing YEP agar plates and incubated for 48 h (DP584) and 72 h (DP553) at 28 °C before the images were captured.

Results and discussion

Chemistry

As outlined in Scheme 1, the target compounds were effectively prepared from hydroxycoumarins **5a**–**b**, which were synthesized using methods reported in literature [37, 38]. The benzylated 3-aminocoumarins **6a**–**b** were achieved by conventional benzylation of the hydroxyl group on C-7 of hydroxycoumarins **5a**–**b** followed by acidic boc-deprotection of the benzylated intermediates to liberate the NH_2 at position 3 of the coumarin nucleus [38, 39]. Subsequently, ferrocenecarboxylic acid was appended to the RHS of the coumarin core via standard amide coupling reaction conditions to generate amides **7a**–**b**.

Initially, the amidation reaction of **6a**–**b** was performed with the common coupling agent, 1-ethyl-3-(3-dimethylaminopropyl)carbodiimide (EDCI); however, the resulting yields were too low (10–18%) to progress to subsequent steps [3]. In attempts to improve the yields, we employed a modified procedure reported by Dunetz et al. that utilises a peptide coupling agent, *n*-propylphosphonic anhydride (T3P®), for

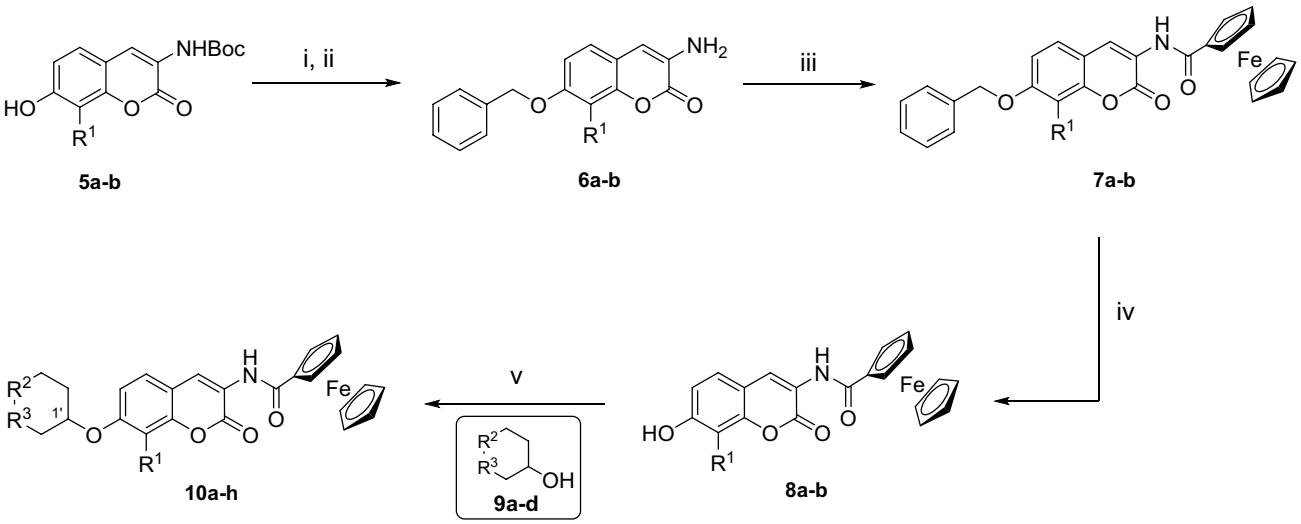

	R^1	R^2	R^3
a	H	NMe	CH_2
b	H	CH_2	NMe
c	Me	NMe	CH_2
d	Me	CH_2	NMe
e	H	NBoc	CH_2
f	H	CH_2	NBoc
g	H	NH	CH_2
h	H	CH_2	NH

Scheme 1 Reagents and conditions: (i) benzyl bromide, K_2CO_3, acetone, 56°C, 3 h; (ii) 4 M HCl in dioxane, r.t., 12 h; (iii) Ferrocene carboxylic acid, 50% T3P®/EtOAc, 1:2 pyridine/$CHCl_3$, 75°C, 24–48 h; (iv) 10 mol % Pd/C, THF, r.t., 12 h; (v) **9a**–**d**, DIAD, PPh_3, THF, 0°C, 5 h; (vi) 10% TFA/DCM, r.t., 12 h

the amidation of epimerization-prone substrates [40]. Thus, refluxing of equimolar amounts of amines (**6a**–**b**) and ferrocene carboxylic acid in 1:2 pyridine/chloroform solution in the presence of two equivalents of the commercially available 50% T3P®/EtOAc solution yielded compounds **7a**–**b** in yields of 68–80%, which was a fourfold improvement compared to the initial EDCI amidation protocol. Subsequently, the target benzylated compounds **7a**–**b** were characterized by ^{1}H and ^{13}C NMR spectroscopic techniques. From the ^{1}H NMR data, the ferrocene protons of compounds **7a**–**b** appeared in the aliphatic region as two triplets and one intense singlet, respectively, at δ 4.84–4.47 ppm and δ 4.26 ppm, confirming successful coupling of ferrocene carboxylic acid to the coumarin nucleus to form the target compounds.

To access the 7-hydroxy novobiocin derivatives **8a**–**b**, compounds **7a**–**b** were stirred under hydrogen atmosphere in THF to remove the benzyl group using 10 mol % palladium on carbon (Pd/C) as a catalyst [39]. Successful benzyl deprotection was confirmed by the disappearance of the signals corresponding to the benzyl group in both ^{1}H and ^{13}C NMR spectra of the products, which were obtained as white solids in 33–96% yields. Having successfully achieved the phenolic derivatives **8a**–**d**, the next step was to pursue the piperidinyl variants **10a**–**f** which were synthesized by coupling piperidinols **9a**–**d** to C-7 of the coumarin nucleus under Mitsunobu reaction conditions [15]. The 3′- and 4′-NMe and -*N*Boc piperidinyl derivatives (**10a**–**f**) were achieved in one step and in modest yields (22–41%). Boc-deprotection of **10e**–**f** by stirring in 10% TFA/DCM solution generated the corresponding NH variants (**10g**–**h**) in excellent yields (95–97%). The methylene protons of the piperidine skeleton were observed as multiplets in the aliphatic region of the ^{1}H NMR spectra of **10a**–**h**, whereas the proton on C-1′ appeared as a broad singlet or multiplet, thus confirming successful attachment of the piperidine unit.

Biological evaluation studies

The synthesized final novobiocin derivatives (**10a**–**h**) and key intermediates, the benzyl (**7a**–**d**) and hydroxyl (**8a**–**d**) series, were screened for in vitro anticancer and antimalarial activity, respectively, against the breast cancer cell line MDA-MB-231 and the chloroquine sensitive (CQS) *P. falciparum* strain, 3D7. These compounds were also evaluated for general human cytotoxicity using the HeLa cell line. The Hsp90 inhibitory activity of the most promising compounds was investigated by means of a yeast assay employing *Saccharomyces* strains that express Hsp90 isoforms from human and *P. falciparum* [36]. Additionally, the effects of these compounds on the levels of Hsp90, Hsp70 (an indirect measure of Hsp90 inhibition) and an obligate Hsp90 client protein, cyclin-dependent kinase 4 (CDK4), were also assessed in MDA-MB-231 cells using Western blot analysis [32, 33]. The parent compound novobiocin (**1**) is not a potent Hsp90 inhibitor, but was included in the biological assays together with the potent inhibitors 17-dimethylaminoethylamino-17-demethoxygeldanamycin (17-DMAG; alvespimycin) and geldanamycin (GA) to determine whether the biological responses of the derivatives are similar to novobiocin, or whether they gain activity more similar to higher affinity Hsp90 inhibitors.

Anticancer activity

In the assay for anticancer activity, paclitaxel, a known anticancer drug, was used as a positive control whilst novobiocin (**1**) was included in the screening assays for reference purposes. The activity of each compound against the MDA-MB-231 breast cell line is presented as a concentration of the compound that suppressed the viability of the cells by half of their initial population, i.e., half-maximal inhibitory concentration (IC_{50}) value. The results are summarised in Table 1.

As illustrated in Table 1, the anticancer activities of compounds in the hydroxyl series (**8a**–**b**) were the most potent in the whole library. With the exception of **10h** (IC_{50} = 108.9 μM), the piperidinyl derivatives (**10a**–**g**) displayed moderate activity with IC_{50} values ranging between 11 and 51 μM. Within this class, the 3′-*N*-methyl analogues (**10b** and **10d**) were almost twice as active as their 4′-*N*-methyl counterparts (**10a** and **10c**), whilst the *N*Boc derivatives (**10e**–**f**) displayed comparable activities of 29.8 and 30.0 μM, respectively. Zhao et al. noted similar trends for organic novobiocin analogues bearing the benzamide chain of **1**, which were tested for antiproliferative effects against SKBr3 and MCF-7 breast cancer cell lines [41]. The NH group (**10g**) also appeared to be tolerated for activity. Methylation of position 8 of the coumarin nucleus is known to be favourable for anticancer activity of novobiocin analogues [4]. This was similarly observed in our results as the 8-methyl derivatives had slightly lower IC_{50} values compared to their variants devoid of the methyl group on C-8 (Table 1). Overall, the derivatives pursued in this study were clearly superior to the parental compound **1** with approximately fourfold improvement in activity (Table 1). Additionally, the replacement of the noviose moiety at C-7 with hydroxy, benzyl and piperidinyl units retained the anticancer activity of the ferrocenyl novobiocin derivatives [16, 17].

Antiplasmodial assay

To establish their antiplasmodial activity, the target compounds and the reference compound, novobiocin (**1**), were subjected to the malaria parasite lactate dehydrogenase (pLDH) assay that was performed in triplicate for each

Table 1 Anticancer and antiplasmodial activities of target compounds against the MDA-MB-231 cancer cell line and 3D7 *P. falciparum* strain, respectively

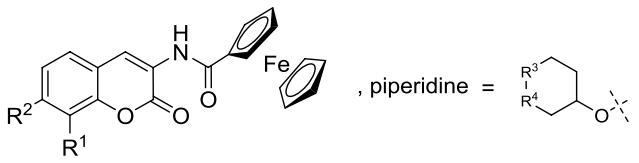

7a-b, **8a-b** and **10a-h**

Entry	Compound	R^1	R^2	R^3	R^4	IC_{50} (μM)	
						MDA-MB-231	3D7
1	**7a**	H	OBn	–	–	182.9	na
2	**7b**	Me	OBn	–	–	41.1	na
3	**8a**	H	OH	–	–	11.7	na
4	**8b**	Me	OH	–	–	29.3	na
5	**10a**	H	piperidine	NMe	CH_2	51.4	7.06
6	**10b**	H	piperidine	CH_2	NMe	47.9	9.16
7	**10c**	Me	piperidine	NMe	CH_2	36.8	0.889
8	**10d**	Me	piperidine	CH_2	NMe	13.8	na
9	**10e**	H	piperidine	*N*Boc	CH_2	29.8	na
10	**10f**	H	piperidine	CH_2	*N*Boc	30.0	na
11	**10g**	H	piperidine	NH	CH_2	11.8	na
12	**10h**	H	piperidine	CH_2	NH	108.9	na
13	**Novobiocin**	–	–	–	–	205.1	na
14	**Paclitaxel**	–	–	–	–	0.029	nd
15	**CQ**	–	–	–	–	nd	0.0102

Activity of compounds is reported as IC_{50} values representing concentrations of the compounds that effected 50% inhibition of cellular growth. Data are expressed as average μM concentration resulting from at least two independent experiments

na not active, *nd* not determined

compound at a concentration of 20 μM. The antiplasmodial screening assay data for the screened compounds is presented in Fig. S1. The compounds were also investigated for general human cytotoxicity using the HeLa cell line to determine if the observed antiplasmodial activity was independent of general cytotoxicity of the compounds. From Fig. S1, three ferrocenyl derivatives **10a**–**c**, which all contain *N*-methyl substituents in the piperidine ring displayed desirable antiplasmodial activity with *P. falciparum* viability reduced to below 25% without substantial HeLa cell cytotoxicity. The data suggest that these compounds were selective for the *P. falciparum* parasite. The rest of the compounds in this series, including parental novobiocin (**1**), were inactive with > 75% *P. falciparum* percentage viability often observed (Fig. S1). In addition, the *N*-methyl group seemed to be permissible for antiplasmodial activity since the three ferrocenyl analogues (**10a**–**c**) with this group exhibited favourable activity.

Following the initial screening data, the most active piperidinyl derivatives were further screened for antiplasmodial activity at varying concentrations to determine their corresponding IC_{50} values (Table 1, Fig. S2). Compounds **10a**–**c** were screened in conjunction with chloroquine (CQ), which was employed as a positive control. The compounds showed moderate activity with IC_{50} values below 10 μM (Table 1, Fig. S2). Most importantly, compound **10c** displayed significant potency in the sub-micromolar range with IC_{50} value of 0.889 μM.

Hsp90 inhibition studies

Having evaluated the compounds for in vitro anticancer and antiplasmodial activity, the next step was to investigate if these compounds act through inhibition of Hsp90. To realize this, *Saccharomyces cerevisiae* (yeast) strains expressing *Homo sapiens* Hsp90β (which is the essential

isoform in humans) [32] and *P. falciparum* Hsp90 isoform were employed to probe the Hsp90 inhibitory activity of the compounds showing the most promising anticancer and antiplasmodial activities. The yeast strains employed were DP584 (expressing *Hs*Hsp90β) and DP553 (expressing *Pf* Hsp90). Compounds **10a** and **10g** were selected as they displayed superior activity against the *P. falciparum* 3D7 strain and the MDA-MB-231 breast cancer cell line, respectively. The known Hsp90 inhibitor, geldanamycin (GA), was included as a positive control and the parental compound novobiocin (**1**) as a reference. For each compound, different yeast densities were plated and incubated with 1 mM of the test compound dissolved in DMSO. The effects of the compounds on yeast growth were visually monitored and the results are presented in Fig. 2a. The white spots indicate the growth of the yeast, where density is proportionate to the growth.

As can be observed from Fig. 2a, GA repressed the growth of the yeast for both strains whereas **10a** and **10g** exerted effects comparable to DMSO, which was used as a negative control in the assay. As a modest Hsp90 inhibitor, novobiocin (**1**) exhibited poor activity against these strains (Fig. 2a). Although **10a** might appear to be slightly effective against DP854 and **10g** against DP553, these effects were in comparison less visible than that of the parental compound **1** on both strains.

In addition, the effect of these compounds on the levels of Hsp90, Hsp70 and kinase CDK4 in MDA-MB-231 cells was compared to known Hsp90 inhibitors 17-DMAG (Alvespimycin) and novobiocin (NOV) (Fig. 2b). CDK4 is a validated Hsp90 client that undergoes degradation upon Hsp90 inhibition [42]. Furthermore, Hsp70 levels can be used as an indirect measure of Hsp90 inhibition due to activation of the heat shock response by *N*-terminal Hsp90 inhibitors [43]. Treatment of cells with the Hsp90 inhibitor 17-DMAG resulted in a significant loss of the obligate Hsp90 client protein, CDK4, and resulted in upregulation in Hsp70 levels without changing Hsp90 levels (Fig. 2b, c). Treatment of the MDA-MB-231 cell line with compounds **10a** and **10g** did not significantly alter the levels of Hsp70 or CDK4, although **10a** appeared to increase the levels of CDK4, while **10g** led to a minor reduction in CDK4 levels (Fig. 2c).

Taken together, and considering that these compounds were significantly more potent than **1**, against the MDA-MB-231 breast cancer cell line and the 3D7 *P. falciparum* strain, a similar trend would be expected against the postulated target Hsp90, as investigated in these assays, if the

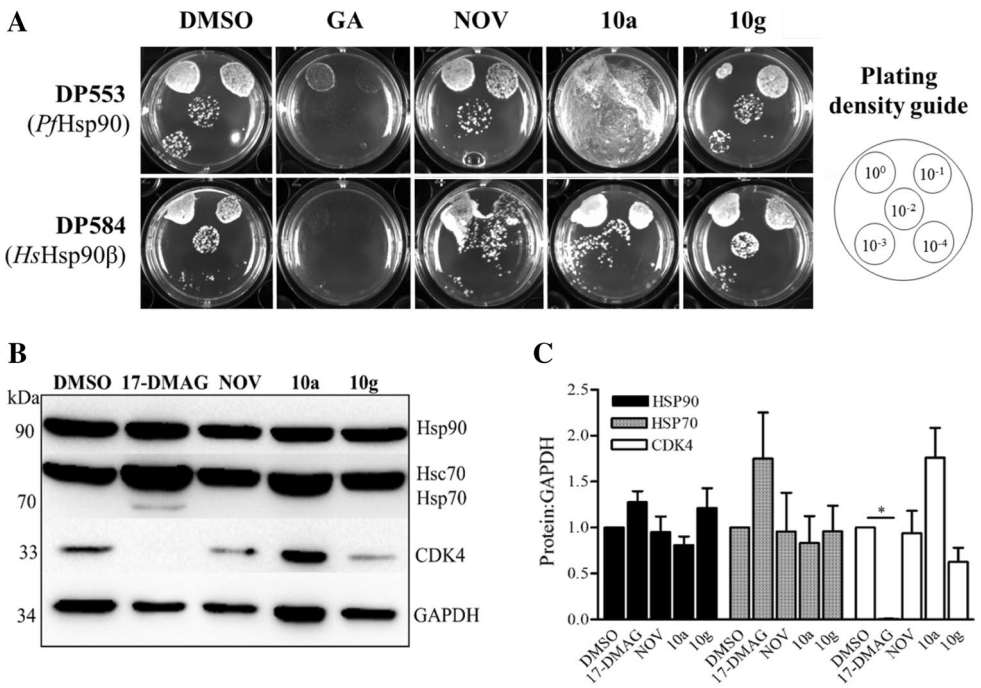

Fig. 2 Hsp90 inhibition assay results for compounds **10a** and **10g**. Analysis of anti-Hsp90 activity of compounds **10a** and **10g** assessing **a** yeast growth assay in strains expressing either *Plasmodium falciparum* or human Hsp90 (DP553 or DP584) in comparison to Hsp90 inhibitors geldanamyin (GA) or novobiocin (NOV). **b** Western blot and **c** densitometry relative to loading control (GAPDH) of levels of Hsp90, Hsp70 or CDK4 in treated MDA-MB-231 cell lysates compared to Hsp90 inhibitors 17-dimethylaminoethylamino-17-demethoxygeldanamycin (17-DMAG; alvespimycin) or NOV. In all cases, DMSO was used as the vehicle control. Data are representative of two independent biological replicates. Statistical significance was determined compared to the DMSO control by two-way ANOVA; $^{*}p < 0.05$

observed activities of these compounds are primarily due to the inhibition of this protein. The data presented (Fig. 2) suggest that there is no correlation between the inhibition of Hsp90 and the observed in vitro anticancer and antiplasmodial activities of the ferrocenyl novobiocin derivatives. The increased toxicity of the ferrocenyl novobiocin derivatives compared to novobiocin could not be explained by increased anti-Hsp90 activity, suggesting that this class of compounds may act on a target other than the Hsp90 to induce the observed activities. In view of the fact that all the organic novobiocin derivatives reported in literature are known to exert anticancer activity through Hsp90 inhibition [44], it is tempting to speculate from our findings that the presence of the ferrocene unit in the novobiocin scaffold switches the target of the derivatives from Hsp90.

Conclusions

Herein, we presented the synthesis of novobiocin–ferrocene conjugates containing simplified structural units (hydroxyl, benzyl and piperidine) in place of the complex noviose motif, which were obtained in moderate yields. The series was investigated for anticancer and antimalarial activity, respectively, using the MDA-MB-231 breast cancer cell line and *P. falciparum* 3D7 strain. In general, the presence of the ferrocene unit was found to favour high potency and selectivity to the novobiocin derivatives evaluated against the breast cancer cell line and the *P. falciparum* parasite. These findings appeared to assert our previous observation that the ferrocene unit imparts beneficial biological effects to novobiocin derivatives. The replacement of the noviose appendage of novobiocin with hydroxy, benzyl and piperidine units seemed to retain the efficacy of the ferrocenyl derivatives. Furthermore, the in vitro anticancer and antiplasmodial activity observed for these derivatives was found to be independent of inhibition of the proposed target, Hsp90.

Acknowledgements The authors would like to acknowledge Rhodes University Sandisa Imbewu (SDK, HCH and ALE) and the National Research Foundation (MM, JNS, ALE and SDK) for financial support. Financial assistance from South African Research Chairs Initiative of the Department of Science and Technology and National Research Foundation of South Africa (Grant No 98566) is also acknowledged (ALE). The South African Medical Research Council (MRC) funded the antiplasmodial bioassay component of the project with funds from National Treasury under its Economic Competitiveness and Support Package.

Compliance with ethical standards

Conflict of interest The authors declare that they have no conflict of interest.

References

1. Marcu MG, Schulte TW, Neckers L (2000) Novobiocin and related coumarins and depletion of heat shock protein 90-dependent signaling proteins. J Natl Cancer Inst 92(3):242–248
2. Burlison JA, Neckers L, Smith AB, Maxwell A, Blagg BS (2006) Novobiocin: redesigning a DNA gyrase inhibitor for selective inhibition of hsp90. J Am Chem Soc 128(48):15529–15536
3. Burlison JA, Avila C, Vielhauer G, Lubbers DJ, Holzbeierlein J, Blagg BS (2008) Development of novobiocin analogues that manifest anti-proliferative activity against several cancer cell lines. J Org Chem 73(6):2130–2137
4. Donnelly AC, Mays JR, Burlison JA, Nelson JT, Vielhauer G, Holzbeierlein J, Blagg BS (2008) The design, synthesis, and evaluation of coumarin ring derivatives of the novobiocin scaffold that exhibit antiproliferative activity. J Org Chem 73(22):8901–8920
5. Young JC, Moarefi I, Hartl FU (2001) Hsp90: a specialized but essential protein-folding tool. J Cell Biol 154(2):267–274
6. Zuehlke A, Johnson JL (2010) Hsp90 and co-chaperones twist the functions of diverse client proteins. Biopolymers 93(3):211–217
7. Holzbeierlein JM, Windsperger A, Vielhauer G (2010) Hsp90: a drug target? Curr Oncol Rep 12(2):95–101
8. Pallavi R, Roy N, Nageshan RK, Talukdar P, Pavithra SR, Reddy R, Venketesh S, Kumar R, Gupta AK, Singh RK (2010) Heat shock protein 90 as a drug target against protozoan infections biochemical characterization of Hsp90 from Plasmodium falciparum and trypanosoma evansi and evaluation of its inhibitor as a candidate drug. J Biol Chem 285(49):37964–37975
9. Kumar R, Musiyenko A, Barik S (2003) The heat shock protein 90 of Plasmodium falciparum and antimalarial activity of its inhibitor, geldanamycin. Malar J 2(1):30
10. Banumathy G, Singh V, Pavithra SR, Tatu U (2003) Heat shock protein 90 function is essential for *Plasmodium falciparum* growth in human erythrocytes. J Biol Chem 278(20):18336–18345
11. Peterson LB, Blagg BS (2009) To fold or not to fold: modulation and consequences of Hsp90 inhibition. Future Med Chem 1(2):267–283
12. Shahinas D, Folefoc A, Pillai DR (2013) Targeting Plasmodium falciparum Hsp90: towards reversing antimalarial resistance. Pathogens 2(1):33–54
13. Le Bras G, Radanyi C, Peyrat J-F, Brion J-D, Alami M, Marsaud V, Stella B, Renoir J-M (2007) New novobiocin analogues as antiproliferative agents in breast cancer cells and potential inhibitors of heat shock protein 90. J Med Chem 50(24):6189–6200
14. Radanyi C, Le Bras G, Marsaud V, Peyrat J-F, Messaoudi S, Catelli M-G, Brion J-D, Alami M, Renoir J-M (2009) Antiproliferative and apoptotic activities of tosylcyclonovobiocic acids as potent heat shock protein 90 inhibitors in human cancer cells. Cancer Lett 274(1):88–94
15. Donnelly AC, Zhao H, Kusuma BR, Blagg BS (2010) Cytotoxic sugar analogues of an optimized novobiocin scaffold. Med Chem Commun 1(2):165–170
16. Zhao H, Donnelly AC, Kusuma BR, Brandt GE, Brown D, Rajewski RA, Vielhauer G, Holzbeierlein J, Cohen MS, Blagg BS (2011) Engineering an antibiotic to fight cancer: optimization of the novobiocin scaffold to produce anti-proliferative agents. J Med Chem 54(11):3839–3853
17. Mbaba M, Mabhula AN, Boel N, Edkins AL, Isaacs M, Hoppe HC, Khanye SD (2017) Ferrocenyl and organic novobiocin derivatives: synthesis and their in vitro biological activity. J Inorg Biochem 172:88–93
18. Raghavan PS, Kumar R, Tatu U (2007) Systems analysis of chaperone networks in the malarial parasite *Plasmodium falciparum*. PLoS Comput Biol 3:e168

19. Wang T, Bisson WH, Mäser P, Scapozza L, Picard D (2014) Differences in conformational dynamics between *Plasmodium falciparum* and human Hsp90 orthologues enable the structure-based discovery of pathogen-selective inhibitors. J Med Chem 57(6):2524–2535
20. Wang T, Mäser P, Picard D (2016) Inhibition of *Plasmodium falciparum* Hsp90 contributes to the antimalarial activities of aminoalcohol-carbazoles. J Med Chem 59(13):6344–6352
21. Bayih AG, Folefoc A, Mohon AN, Eagon S, Anderson M, Pillai DR (2016) In vitro and in vivo anti-malarial activity of novel harmine-analog heat shock protein 90 inhibitors: a possible partner for artemisinin. Malar J 15(1):579
22. Divo A, Sartorelli A, Patton C, Bia F (1988) Activity of fluoroquinolone antibiotics against *Plasmodium falciparum* in vitro. Antimicrob Agents Chemother 32(8):1182–1186
23. Ram ER, Kumar A, Biswas S, Kumar A, Chaubey S, Siddiqi MI, Habib S (2007) Nuclear gyrB encodes a functional subunit of the *Plasmodium falciparum* gyrase that is involved in apicoplast DNA replication. Mol Biochem Parasitol 154(1):30–39
24. Chavain N, Biot C (2010) Organometallic complexes: new tools for chemotherapy. Curr Med Chem 17(25):2729–2745
25. Gasser G, Metzler-Nolte N (2012) The potential of organometallic complexes in medicinal chemistry. Curr Opin Chem Biol 16(1–2):84–91
26. Hartinger CG, Metzler-Nolte N, Dyson PJ (2012) Challenges and opportunities in the development of organometallic anticancer drugs. Organometallics 31(16):5677–5685
27. Patra M, Gasser G (2017) The medicinal chemistry of ferrocene and its derivatives. Nat Rev Chem 1(9):0066
28. Kowalski K (2018) Recent developments in the chemistry of ferrocenyl secondary natural product conjugates. Coord Chem Rev 366:91–108
29. To evaluate the efficacy of a single dose regimen of ferroquine and artefenomel in adults and children with uncomplicated *Plasmodium falciparum* Malaria (FALCI) (2018) US National Library of Medicine. https://clinicaltrials.gov/ct2/show/NCT02497612. Accessed 28 October 2018
30. Top S, Tang J, Vessières A, Carrez D, Provot C, Jaouen G (1996) Ferrocenyl hydroxytamoxifen: a prototype for a new range of oestradiol receptor site-directed cytotoxics. Chem Commun 8:955–956
31. Jaouen G, Vessières A, Top S (2015) Ferrocifen type anti cancer drugs. Chem Soc Rev 44(24):8802–8817
32. Laemmli UK (1970) Cleavage of structural proteins during the assembly of the head of bacteriophage T4. Nature 227(5259):680–685
33. Towbin H, Staehelin T, Gordon J (1979) Electrophoretic transfer of proteins from polyacrylamide gels to nitrocellulose sheets: procedure and some applications. Proc Natl Acad Sci USA 76(9):4350–4354
34. Lunga MJ, Chisango RL, Weyers C, Isaacs M, Taylor D, Edkins AL, Khanye SD, Hoppe HC, Veale C (2018) Expanding the SAR of non-toxic antiplasmodial indolyl-3-ethanone ethers and thioethers. ChemMedChem 13:1353–1362
35. Oderinlo OO, Tukulula M, Isaacs M, Hoppe HC, Taylor D, Smith VJ, Khanye SD (2018) New thiazolidine-2, 4-dione derivatives combined with organometallic ferrocene: Synthesis, structure and antiparasitic activity. Appl Organomet Chem 32(7):e4385
36. Wider D, Péli-Gulli M-P, Briand P-A, Tatu U, Picard D (2009) The complementation of yeast with human or *Plasmodium falciparum* Hsp90 confers differential inhibitor sensitivities. Mol Biochem Parasitol 164(2):147–152
37. Mendelson WL, Hayden S (1996) Preparation of 2,4-dihydroxybenzaldehyde by the Vilsmeier-Haack Reaction. Synth Commun 26(3):603–610
38. Kudale AA, Kendall J, Warford CC, Wilkins ND, Bodwell GJ (2007) Hydrolysis-free synthesis of 3-aminocoumarins. Tetrahedron Lett 48(29):5077–5080
39. Nicolaou K, Bunnage ME, Koide K (1994) Total synthesis of balanol. J Am Chem Soc 116(18):8402–8403
40. Dunetz JR, Xiang Y, Baldwin A, Ringling J (2011) General and scalable amide bond formation with epimerization-prone substrates using T3P and pyridine. Org Lett 13(19):5048–5051
41. Zhao H, Reddy Kusuma B, Blagg BS (2010) Synthesis and evaluation of noviose replacements on novobiocin that manifest antiproliferative activity. ACS Med Chem Lett 1(7):311–315
42. Theodoraki MA, Caplan AJ (2012) Quality control and fate determination of Hsp90 client proteins. BBA Mol Cell Res 1823(3):683–688
43. Sittler A, Lurz R, Lueder G, Priller J, Hayer-Hartl MK, Hartl FU, Lehrach H, Wanker EE (2001) Geldanamycin activates a heat shock response and inhibits huntingtin aggregation in a cell culture model of Huntington's disease. Hum Mol Genet 10(12):1307–1315
44. Dlugosz A, Janecka A (2017) Novobiocin analogs as potential anticancer agents. Mini Rev Med Chem 17(9):728–733

Affiliations

Mziyanda Mbaba[1] · Jo-Anne de la Mare[2,3,4] · Jason N. Sterrenberg[2,3] · Deborah Kajewole[2,3] · Shantal Maharaj[2,3] · Adrienne L. Edkins[2,3,4] · Michelle Isaacs[4] · Heinrich C. Hoppe[2,3,4] · Setshaba D. Khanye[1,4,5]

1 Department of Chemistry, Faculty of Science, Rhodes University, Grahamstown 6140, South Africa

2 Department of Biochemistry and Microbiology, Faculty of Science, Rhodes University, Grahamstown 6140, South Africa

3 Biomedical Biotechnology Research Unit (BioBRU), Rhodes University, Grahamstown 6140, South Africa

4 Centre for Chemico- and Biomedical Research, Rhodes University, Grahamstown 6140, South Africa

5 Faculty of Pharmacy, Rhodes University, Grahamstown 6140, South Africa